Bioorganic & Medicinal Chemistry Letters 18 (2008) 3711–3715

Contents lists available at ScienceDirect

Bioorganic & Medicinal Chemistry Letters

journal homepage: www.elsevier.com/locate/bmcl

# Discovery and biological evaluation of novel α-glucosidase inhibitors with in vivo antidiabetic effect

Hwangseo Park [a,*], Kyo Yeol Hwang [b], Young Hoon Kim [b], Kyung Hwan Oh [b], Jae Yeon Lee [b], Keun Kim [b,*]

[a] Department of Bioscience and Biotechnology, Sejong University, 98 Kunja-Dong, Kwangjin-Ku, Seoul 143-747, Republic of Korea
[b] Department of Bioscience and Biotechnology, The University of Suwon, San 2-2 Wau-ri, Bongdam-eup, Hwaseong-si, Gyeonggi-do 445-743, Republic of Korea

ARTICLE INFO

*Article history:*
Received 21 April 2008
Revised 14 May 2008
Accepted 15 May 2008
Available online 20 May 2008

*Keywords:*
Virtual screening
α-Glucosidase
Inhibitor
Diabetes
Antidiabetic activity

ABSTRACT

Discovery of α-glucosidase inhibitors has been actively pursued with the aim to develop therapeutics for the treatment of diabetes and the other carbohydrate-mediated diseases. We have identified four novel α-glucosidase inhibitors by means of a drug design protocol involving the structure-based virtual screening under consideration of the effects of ligand solvation in the scoring function and in vitro enzyme assay. Because the newly identified inhibitors reveal in vivo antidiabetic activity as well as a significant potency with more than 70% inhibition of the catalytic activity of α-glucosidase at 50 μM, all of them seem to deserve further development to discover new drugs for diabetes. Structural features relevant to the interactions of the newly identified inhibitors with the active site residues of α-glucosidase are discussed in detail.



Glucosidases are responsible for the catalytic cleavage of a glycosidic bond in the digestive process of carbohydrates with specificity depending on the number of monosaccharides, the position of cleavage site, and the configuration of the hydroxyl groups in the substrate.[1] α- and β-glucosidases are most extensively studied and are known to catalyze the hydrolysis of the glycosidic bonds involving a terminal glucose at the cleavage site.[2] Of the two popular glucosidases, α-glucosidase (EC 3.2.1.20) has drawn a special interest of the pharmaceutical research community because it was shown that the inhibition of its catalytic activity led to the retardation of glucose absorption and the decrease in postprandial blood glucose level.[3–5] This indicates that effective α-glucosidase inhibitors may serve as chemotherapeutic agents for clinic use in the treatment of diabetes and obesity. The catalytic role in digesting carbohydrate substrates also makes α-glucosidase a therapeutic target for the other carbohydrate-mediated diseases including cancer,[6] viral infections,[7,8] and hepatitis.[9]

Since the discovery of acarbose (Figure 1), that is the first member of α-glucosidase inhibitors approved for the treatment of type 2 diabetes,[10] a variety of α-glucosidase inhibitors have been discovered as recently reviewed in an extensive fashion.[11] These include transition state analogues,[12] newly identified synthetic compounds,[13–21] and natural products isolated from a variety of species.[22–25] Most of the α-glucosidase inhibitors reported in the literature stem from either the isolation of new scaffolds by high throughput screening or the generation of the improved derivatives of pre-existing inhibitor scaffolds. So far the structural investigations of α-glucosidases have lagged behind the mechanistic and pharmacological studies. Indeed, structural information of α-glucosidases has been limited to those of a few bacterial strains only in ligand-free forms.[26,27] The lack of structural information about the nature of the interactions between α-glucosidases and the inhibitors has thus made it a difficult task to discover good lead compounds based on the structure-based inhibitor design.

Recently we have identified several α-glucosidase inhibitors based on a drug-design protocol involving homology modeling, virtual screening with docking simulations, and in vitro enzyme assay.[28] In this study, we also apply a structure-based virtual screening with the aim to discover the new α-glucosidase inhibitors that can reduce the postglandal blood glucose level in vivo. The present virtual screening approach differs from the previous one in that a putative ligand is scored with the most populated binding mode instead of the lowest binding free energy hit. This may have an effect of increasing the hit rate in enzyme assay because the binding free energy function in itself is insufficient to ensure the successful virtual screening.[29] Another characteristic feature of the present virtual screening lies in the implementation of an accurate solvation model in the scoring function. It will be shown that the present virtual screening approach can be useful for enriching a chemical library with the molecules that are likely to have desired biological activities.

We used the AutoDock program[30] in the structure-based virtual screening of α-glucosidase inhibitors because the outperformance of its scoring function over those of the others had been shown

* Corresponding authors. Tel.: +82 2 3408 3766; fax: +82 2 3408 4334 (H. Park); tel./fax: +82 31 220 2344 (K. Kim).
*E-mail addresses:* hspark@sejong.ac.kr (H. Park), kkim@suwon.ac.kr (K. Kim).

0960-894X/$ - see front matter © 2008 Elsevier Ltd. All rights reserved.
doi:10.1016/j.bmcl.2008.05.056

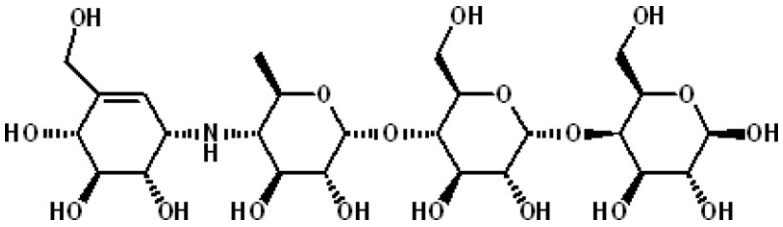

**Figure 1.** Chemical structure of acarbose.

in several target proteins.[31] The atomic coordinates of α-glucosidase obtained from the homology modeling were used as the receptor model in the virtual screening with docking simulations. A special attention was paid to assign the protonation states of the ionizable Asp, Glu, His, and Lys residues. The side chains of Asp and Glu residues were assumed to be neutral if one of their carboxylate oxygens pointed toward a hydrogen-bond accepting group including the backbone aminocarbonyl oxygen at a distance within 3.5 Å, a generally accepted distance limit for a hydrogen bond of moderate strength.[32] Similarly, the side chains of Lys residues were protonated unless the NZ atom was in a close proximity of a hydrogen-bond donating group. The same procedure was also applied to determine the protonation states of ND and NE atoms in the side chains of His residues.

The docking library for α-glucosidase comprising about 85,000 compounds was constructed from the latest version of the Interbioscreen chemical database (http://www.ibscreen.com) containing approximately 30,000 natural and 320,000 synthetic compounds. This selection was based on the drug-like filters that adopt only the compounds with physicochemical properties of potential drug candidates.[33] All of the compounds in the docking library were then subjected to the Corina program to generate three-dimensional coordinates, followed by the assignment of Gasteiger-Marsilli atomic charges.[34] Docking simulations were then carried out in the active site of α-glucosidase to score and rank the compounds according to the calculated binding free energy of the most populated binding configurations.

In the actual docking simulation of the compounds in the docking library, we used the empirical scoring function improved by the implementation of a new solvation model for a compound. The modified scoring function has the following form:

$$\Delta G_{\text{bind}}^{\text{aq}} = W_{vdW}\sum_{i=1}\sum_{j>i}\left(\frac{A_{ij}}{r_{ij}^{12}}-\frac{B_{ij}}{r_{ij}^{6}}\right) + W_{\text{hbond}}\sum_{i=1}\times\sum_{j>i}E(t)\left(\frac{C_{ij}}{r_{ij}^{12}}-\frac{D_{ij}}{r_{ij}^{10}}\right) + W_{\text{elec}}\sum_{i=1}\sum_{j>i}\frac{q_iq_j}{\varepsilon(r_{ij})r_{ij}} + W_{\text{tor}}N_{\text{tor}} + W_{\text{sol}}\sum_{i=1}S_i\left(Occ_i^{\max}-\sum_{j>i}V_j\text{de}^{-\frac{r_{ij}^2}{2\sigma^2}}\right), \quad (1)$$

where $W_{vdW}$, $W_{\text{hbond}}$, $W_{\text{elec}}$, $W_{\text{tor}}$, and $W_{\text{sol}}$ are the weighting factors of van der Waals, hydrogen bond, electrostatic interactions, torsional term, and desolvation energy of an inhibitor, respectively. $r_{ij}$ represents the interatomic distance, and $A_{ij}$, $B_{ij}$, $C_{ij}$, and $D_{ij}$ are related to the depths of the potential energy well and the equilibrium separations between the two atoms. The hydrogen bond term has an additional weighting factor, $E(t)$, representing the angle-dependent directionality. Cubic equation approach was applied to obtain the dielectric constant required in computing the interatomic electrostatic interactions between α-glucosidase and a ligand molecule.[35] In the entropic term, $N_{tor}$ is the number of $sp^3$ bonds in the ligand. In the desolvation term, $S_i$ and $V_i$ are the solvation parameter and the fragmental volume of atom $i$,[36] respectively, while $Occ_i^{\max}$ stands for the maximum atomic occupancy. In the calculation of molecular solvation free energy term in Eq. 1, we used the atomic parameters recently developed by Kang et al.[37] because those of the atoms other than carbon were unavailable in the current version of AutoDock. This modification of the solvation free energy term is expected to increase the accuracy in virtual screening, because the underestimation of ligand solvation often leads to the overestimation of the binding affinity of a ligand with many polar atoms.[38]

Docking simulation of a compound in the library started with the calculation of the three-dimensional grids of interaction energy for all of the possible atom types present in library. These uniquely defined potential grids for the receptor protein were then used in common for docking simulations of all compounds in the library. As the center of the common grids in the active site, we used the center of mass coordinates of the docked structure of the probe molecule, acarbose, whose binding mode had been known in the active site of 4-α-glucanotransferase that is closely similar in structure to the template (oligo-1,6-glucosidase) used in the homology modeling.[39] The calculated grid maps were of dimension 61 × 61 × 61 points with the spacing of 0.375 Å, yielding a receptor model that includes atoms within 22.9 Å of the grid center. For each compound in the library, 10 docking runs were performed with the initial population of 50 individuals. Of the conformations obtained from 10 docking runs, those clustered together have similar binding modes differing by less than 1.5 Å in positional root-mean-square deviation. The most populated binding configuration of the enzyme-inhibitor complex was then selected for further analysis.

As widely used, the commercially available α-glucosidase from baker's yeast (Sigma, G5003) was selected as the target protein in this study using *p*-nitrophenyl-α-D-glucopyranoside (Sigma, N1377) as the substrate. The compounds selected from the precedent virtual screening were purchased from InterBioScreen Ltd. and dissolved in DMSO. The reason for this choice for solvent lies in that most of the test compounds were soluble and maintained stable in DMSO. The enzyme and the substrate were dissolved in 0.07 M potassium phosphate buffer with pH 6.8. Then, the enzymatic reaction mixture composed of 100 μl α-glucosidase (0.1 U/ml), 99 μl of 5 mM substrate, and 1 μl (10 mM/ml DMSO) of test compound was incubated at 37 °C for 30 min. The inhibitory activity of each test compound was determined by measuring the remaining activity of α-glucosidase at the concentration of 50 μM. The enzymatic activity was measured by the amount of the released product, *p*-nitrophenol, that was detected by spectrophotometer at the wavelength of 415 nm. For all test compounds, the inhibition assay was performed in duplicates.

Parturient female rats (Sprague–Dawley) were housed in a temperature-controlled room (24 ± 2 °C) under artificial illumination (12 h light/dark cycle) and at 55 ± 5% relative humidity. The rats were maintained on a standard pellet diet and water ad libitum. Newly born male rats were used to induce experimental diabetes. Diabetes was induced by two times of intraperitonial injection of 40 mg streptozotocin (STZ; Sigma, S-0313) per kg body weight freshly dissolved in 100 μl of ice-cold 0.1 M citrate buffer (pH 4.5) at 2 and 4 days after birth. Five-week old rats weighing

180–190 g were divided into six groups ($n = 4$): STZ control, acarbose, compound **1**, compound **2**, compounds **3** and compound **4**. After the rats were fasted for 24 h, 1 ml of each chemical maintained at 10 mM in saline solution was administered by oral route to each group of rats, which was immediately followed by the oral administration of 1.5 g/kg of corn starch. Blood was then withdrawn from the rat tail vein at 0, 30, 60, 90 and 120 min post-administration. The blood glucose levels were measured by glucose-dye-oxidoreductase test strips (Accu-Check Active, Roche, Germany).

The α-glucosidase from baker's yeast was selected as the target protein because it had been used most extensively in biological assays to evaluate the newly discovered α-glucosidase inhibitors. Of the 85,000 compounds subject to the virtual screening, 100 top-scored compounds were selected as virtual hits. Ninety-four of them were available from the compound supplier and were tested for inhibitory activity by in vitro enzyme assay. Eight of the 94 screened compounds reveal more than 50% inhibition at the concentration of 50 μM. The inhibitory activities and the chemical structures of the newly identified inhibitors exhibiting more than 70% inhibition of α-glucosidase activity are shown in Table 1 and Figure 2, respectively. These inhibition assays were done in duplicates at the concentration of 50 μM using acarbose as a reference.

**Table 1**
Inhibitory activities of **1**–**4** for α-glucosidase

| Compounds | % inhibition at 50 μM |
|---|---|
| Acarbose | 88.1 ± 5.7 |
| **1** | 88.7 ± 3.3 |
| **2** | 86.0 ± 4.8 |
| **3** | 78.9 ± 5.1 |
| **4** | 75.2 ± 4.6 |

We note that compounds **1** and **2** are as potent as the reference compound in inhibiting the activity of α-glucosidase and possess a common 5-[1-(2-phenoxyethyl)-1 *H*-pyrrol-2-ylmethylene]-1-phenylpyrimidine-2,4,6(1*H*, 3*H*,5*H*)-trione scaffold. **3** and **4** reveal a similar inhibitory activity of 75–80% inhibition of α-glucosidase activity, either of which may be viewed as an independent inhibitor scaffold. The four inhibitors shown in Figure 2 can thus be divided into three structural classes. To the best of our knowledge, all of these compounds have not been reported as α-glucosidase inhibitors so far. It is also noteworthy that none of the four compounds was included in the hit compounds of the previous virtual screening that uses the lowest binding free energy hit in the scoring.[28] This indicates the usefulness of scoring with the most populated binding mode in virtual screening α-glucosidase inhibitors. Judging from the potency and the structural diversity, all of the newly identified inhibitor scaffolds seem to deserve further development by structure-activity relationship (SAR) methods to optimize their inhibitory activities.

To obtain structural insight into the inhibitory mechanisms for the identified inhibitors of α-glucosidase, their binding modes in the active site were investigated using the AutoDock program in comparison with that of the known inhibitor acarbose. Figure 3 shows the best-scored AutoDock conformations of acarbose, **1**, and **3** in the active site gorge of α-glucosidase. As revealed by the superposition of the docked structures, all of the inhibitors seem to be stabilized through the interactions with the two catalytic residues, Glu276 and Asp349. In order to examine the possibility of the allosteric inhibition of α-glucosidase by the inhibitors, docking simulations were carried out with the grid maps for the receptor model so as to include the entire part of α-glucosidase. However, the binding configuration in which an inhibitor resides outside the active site was observed neither for the new inhibitors nor for acarbose. These results support the possibil-

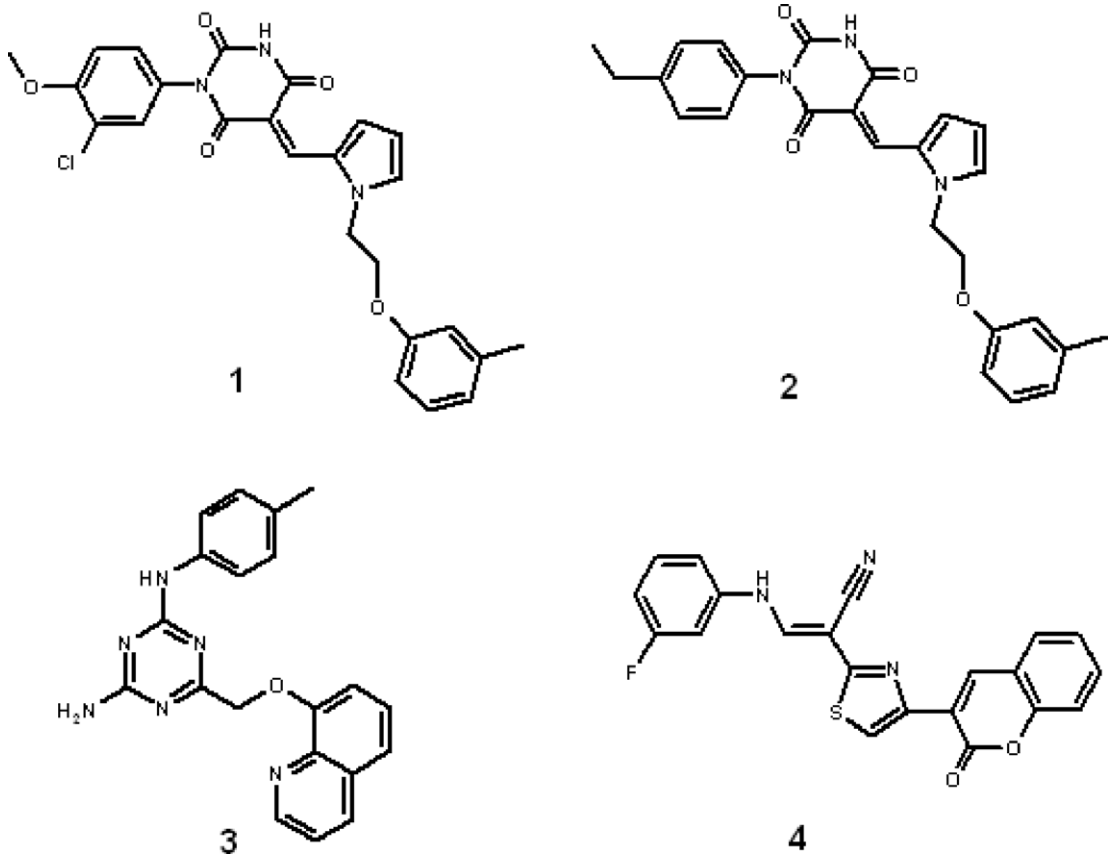


**Figure 2.** Chemical structures of the newly identified α-glucosidase inhibitors.

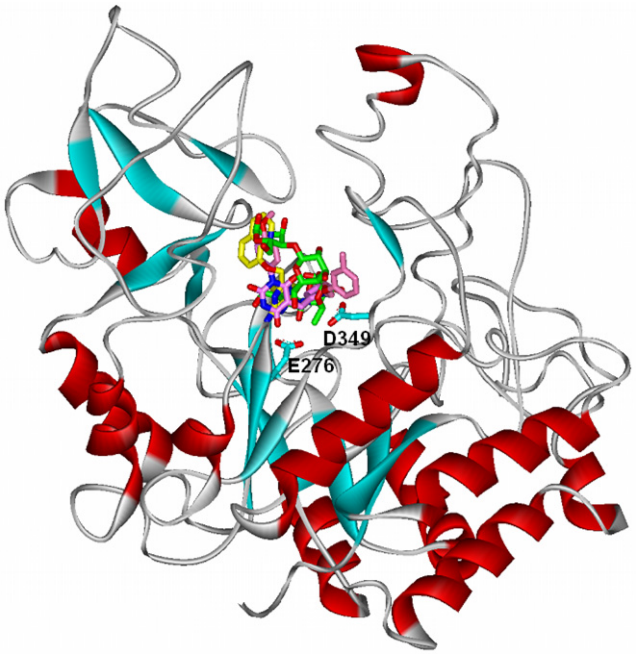


**Figure 3.** Comparative view of the binding modes of acarbose, **1**, and **3** in the active site of α-glucosidase. Carbon atoms of the catalytic residues, acarbose, **1**, and **3** are indicated in cyan, green, pink, and yellow, respectively.

ity that the inhibitors would impair the catalytic activity of α-glucosidase through the specific binding in the active site.

The calculated binding mode of **1** in the active site of α-glucosidase is shown in Figure 4. We note that the pyrimidine-2,4,6-trione moiety of **1** resides in the vicinity of the catalytic residue Glu276 with one of its amidic nitrogens donating a hydrogen bond to the side chain of Thr215. The proximity to the catalytic residue with the hydrogen-bond stabilization indicates that the pyrimidine-2,4,6-trione moiety can serve as an effective surrogate for the terminal monosaccharide of a carbohydrate substrate. A stable hydrogen bond is also established between the terminal methoxy group of **1** and the side chain hydroxy group of Ser244. This hydrogen bond seems to be positioned by a face-to-edge hydrophobic interaction of the adjacent phenyl ring with the side chain of Phe157. **1** can be further stabilized in the active site by the hydrophobic interactions of its aromatic rings with the nonpolar residues including Phe177, Leu218, Leu237, Phe300, and Phe311. Judging from such structural features, **1** should be capable of inhibiting the catalytic action of α-glucosidase by binding in the active site through the establishment of the multiple hydrogen bonds and hydrophobic interactions in a cooperative fashion.

Figure 5 shows the most populated binding mode of **3** in the active site of α-glucosidase. The binding mode of **3** differs from that of **1** in that the hydrogen bond between Thr215 and the inhibitor is not observed. In the calculated α-glucosidase-**3** complex, the role of a surrogate for the terminal monosaccharide of a substrate seems to be played by the[1,3,5]triazine-2,4-diamine group that donates a hydrogen bond to the catalytic residue Glu276. The importance of the capability to form a hydrogen bond with the catalytic residue in the inhibition of glucosidase activity was also demonstrated in recent computational studies.[40] As in the α-glucosidase-**1** complex, the side chain hydroxyl group of Ser244 serves as a hydrogen bond donor with respect to an oxygen atom of **3**. Another characteristic feature that discriminates the binding mode of **3** from that of **1** lies in that the former is stabilized in the active site by less nonpolar side chains than the latter. Because the number of hydrogen bonds is the same in the two complexes, the weakening of the hydrophobic interactions should be responsible for the lower inhibitory activity of **3** than **1**.

In order to investigate the in vivo antidiabetic activity of the newly identified α-glucosidase inhibitors, acute single dose 120-min time-course experiment was carried out using male streptozotocin (STZ) diabetic rats. The blood glucose level increases from 68.2 ± 6.1 in normal rats to 116.9 ± 8.7 mg/dl in the measurement made immediately after the treatment of STZ, and up to 332.7 ± 24.1 mg/dl after 60 min. This significant increase in blood glucose level may serve as evidence for the occurrence of diabetes in STZ rats. Compounds **1-4** were then tested for antidiabetic activity along with acarbose that was used as a standard. The test and standard compounds suspended in saline solution were orally administered to the respective groups consisting of four STZ rats ($n = 4$), which was followed by the blood sampling from rat tail at 30, 60, 90, and 120 min. The blood glucose levels were then measured at each time interval, and the results are summarized in Figure 6.

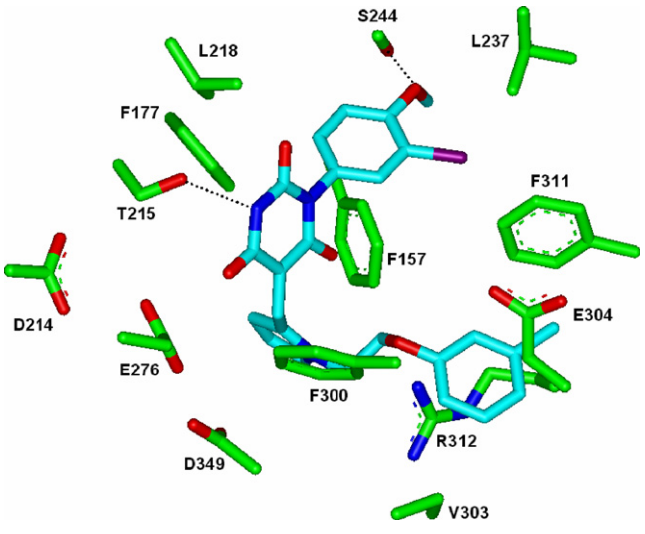


**Figure 4.** Binding mode of **1** in the active site of α-glucosidase. Carbon atoms of the protein and the ligand are indicated in green and cyan, respectively. Each dotted line indicates a hydrogen bond.

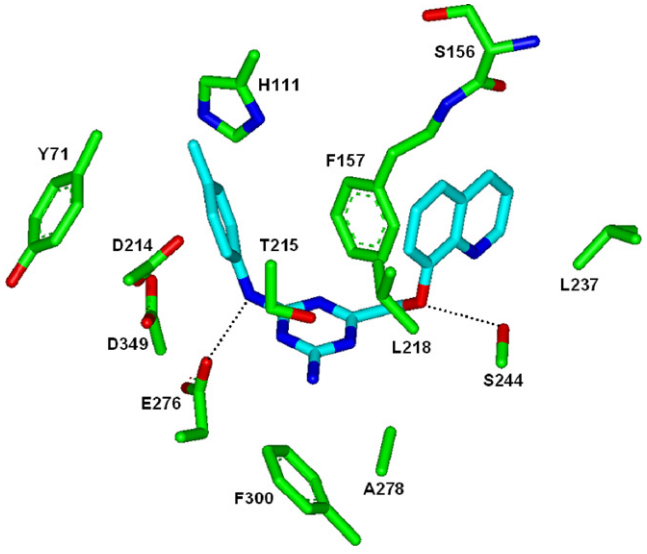


**Figure 5.** Binding mode of **3** in the active site of α-glucosidase. Carbon atoms of the protein and the ligand are indicated in green and cyan, respectively. Each dotted line indicates a hydrogen bond.

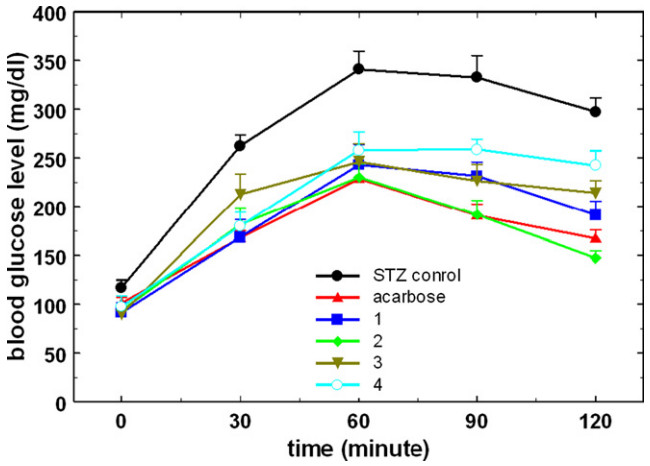


**Figure 6.** Time evolutions of the serum glucose levels after single oral administration of various compounds to STZ diabetic rats. Each error bar indicates the standard deviation measured over the four rats belonging to the same group.

We note that all of the α-glucosidase inhibitors identified in this work and the standard compound (acarbose) exhibit antidiabetic activity with 20-35% decrease in serum glucose levels at 60 min after administration of the compounds. Consistent with the in vitro enzyme assay results for the inhibition of α-glucosidase, compounds **1** and **2** reveal a little higher antidiabetic effect than **3** and **4**. Despite the similar in vitro inhibitory activity against α-glucosidase between **1** and **2**, however, the substitution of an ethyl group of the terminal phenyl ring in **2** for the methoxy and chlorine in **1** leads to 5% and 23% decreases in serum glucose level at 60 and 120 min, respectively. As a result, **2** exhibits a comparable in vivo antidiabetic activity to acarbose. The improvement of ADME properties in going from **1** to **2** can be invoked to explain the difference in the in vivo antidiabetic activity because the inhibitory activities against α-glucosidase are similar. Judging from the in vivo antidiabetic activities as well as the in vitro inhibitory activity for α-glucosidase, compounds **1–4** seem to be able to serve as a new starting point for the discovery of new oral hypoglycemic agents.

In conclusion, we have identified four new novel inhibitors of α-glucosidase by applying a computer-aided drug-design protocol involving the structure-based virtual screening with docking simulations under consideration of the effects of ligand solvation in the scoring function. These inhibitors reveal in vivo antidiabetic activity as well as a significant in vitro potency. Therefore, they seem to deserve further development to discover new drugs for diabetes. Detailed binding mode analyses with docking simulation show that the inhibitors can be stabilized in the active site through the formation of multiple hydrogen bonds with catalytic residues and the establishment of hydrophobic contacts in a cooperative fashion.

## Acknowledgment

The authors thank Prof. Olson at Scripps Research Institute for providing the AutoDock 3.0.5 program.

## References and notes

1. Kimura, A.; Lee, J.-H.; Lee, I.-S.; Lee, H.-S.; Park, K.-H.; Chiba, S.; Kim, D. *Carbohydr. Res.* **2004**, *339*, 1035.
2. Heightman, T. D.; Vasella, A. T. *Angew. Chem. Int. Ed.* **1999**, *38*, 750.
3. Robinson, K. M.; Begovic, M. E.; Rhinehart, B. L.; Heineke, E. W.; Ducep, J. B.; Kastner, P. R.; Marshall, F. N.; Danzin, C. *Diabetes* **1991**, *40*, 825.
4. Braun, C.; Brayer, G. D.; Withers, S. G. *J. Biol. Chem.* **1995**, *270*, 26778.
5. Dwek, R. A.; Butters, T. D.; Platt, F. M.; Zitzmann, N. *Nature Rev. Drug Discov.* **2002**, *1*, 65.
6. Humphries, M. J.; Matsumoto, K.; White, S. L.; Olden, K. *Cancer Res.* **1986**, *46*, 5215.
7. Mehta, A.; Zitzmann, N.; Rudd, P. M.; Block, T. M.; Dwek, R. A. *FEBS Lett.* **1998**, *430*, 17.
8. Karpas, A.; Fleet, G. W. J.; Dwek, R. A.; Petursson, S.; Namgoong, S. K.; Ramsden, N. G.; Jacob, G. S.; Rademacher, T. W. *Proc. Natl. Acad. Sci. U.S.A.* **1988**, *85*, 9229.
9. Zitzmann, N.; Mehta, A. S.; Carrouee, S.; Butters, T. D.; Platt, F. M.; McCauley, J.; Blumberg, B. S.; Dwek, R. A.; Block, T. M. *Proc. Natl. Acad. Sci. U.S.A.* **1999**, *96*, 11878.
10. Yee, H. S.; Fong, N. T. *Pharmacotherapy* **1996**, *16*, 792.
11. de Melo, E. B.; Gomes, A. S.; Carvalho, I. *Tetrahedron* **2006**, *62*, 10277.
12. Lillelund, V. H.; Jensen, H. H.; Liang, X.; Bols, M. *Chem. Rev.* **2002**, *102*, 515.
13. Gao, H.; Kawabata, J. *Bioorg. Med. Chem. Lett.* **2008**, *18*, 812.
14. Xu, H.-W.; Dai, G.-F.; Liu, G.-Z.; Wang, J.-F.; Liu, H.-M. *Bioorg. Med. Chem.* **2007**, *15*, 4247.
15. Tanabe, G.; Yoshikai, K.; Hatanaka, T.; Yaamamoto, M.; Shao, Y.; Minematsu, T.; Muraoka, O.; Wang, T.; Matsuda, H.; Yoshikawa, M. *Bioorg. Med. Chem.* **2007**, *15*, 3926.
16. Liu, Y.; Ma, L.; Chen, W.-H.; Wang, B.; Xu, Z.-L. *Bioorg. Med. Chem.* **2007**, *15*, 2810.
17. Pandey, J.; Dwivedi, N.; Singh, N.; Srivastava, A. K.; Tamarkar, A.; Tripathi, R. P. *Bioorg. Med. Chem. Lett.* **2007**, *17*, 1321.
18. Hakamata, W.; Nakanishi, I.; Masuda, Y.; Shimizu, T.; Higuchi, H.; Nakamura, Y.; Saito, S.; Urano, S.; Oku, T.; Ozawa, T.; Ikota, N.; Miyata, N.; Okuda, H.; Fukuhara, K. *J. Am. Chem. Soc.* **2006**, *128*, 6524.
19. Dai, G.-F.; Xu, H.-W.; Wang, J.-F.; Liu, F.-W.; Liu, H.-M. *Bioorg. Med. Chem. Lett.* **2006**, *16*, 2710.
20. Liu, H.; Sim, L.; Rose, D. R.; Pinto, B. M. *J. Org. Chem.* **2006**, *71*, 3007.
21. Seo, W. D.; Kim, J. H.; Kang, J. E.; Ryu, H. W.; Curtis-Long, M. J.; Lee, H. S.; Yang, M. S.; Park, K. H. *Bioorg. Med. Chem. Lett.* **2005**, *15*, 5514.
22. Luo, J.-G.; Wang, X.-B.; Ma, L.; Kong, L.-Y. *Bioorg. Med. Chem. Lett.* **2007**, *17*, 4460.
23. Saludes, J. P.; Lievens, S. C.; Molinski, T. F. *J. Nat. Prod.* **2007**, *70*, 436.
24. Du, Z.-Y.; Liu, R.-R.; Shao, W.-Y.; Mao, X. P.; Ma, L.; Gu, L.-Q.; Huang, Z.-S.; Chan, A. S. C. *Eur. J. Med. Chem.* **2006**, *41*, 213.
25. Gao, H.; Kawabata, J. *Bioorg. Med. Chem.* **2005**, *13*, 1661.
26. Lodge, J. A.; Maier, T.; Liebl, W.; Hoffmann, V.; Sträter, N. *J. Biol. Chem.* **2003**, *278*, 19151.
27. Rajan, S. S.; Yang, X.; Collart, F.; Yip, V. L. Y.; Withers, S. G.; Varrot, A.; Thompson, J.; Davies, G. J.; Anderson, W. F. *Structure* **2004**, *12*, 1619.
28. Park, H.; Hwang, K. Y.; Oh, K. H.; Kim, Y. H.; Lee, J. Y.; Kim, K. *Bioorg. Med. Chem.* **2008**, *16*, 284.
29. Warren, G. L.; Andrews, C. W.; Capelli, A.-M.; Clarke, B.; LaLonde, J.; Lambert, M. H.; Lindvall, M.; Nevins, N.; Semus, S. F.; Senger, S.; Tedesco, G.; Wall, I. D.; Woolven, J. M.; Peishoff, C. E.; Head, M. S. *J. Med. Chem.* **2006**, *49*, 5912.
30. Morris, G. M.; Goodsell, D. S.; Halliday, R. S.; Huey, R.; Hart, W. E.; Belew, R. K.; Olson, A. J. *J. Comput. Chem.* **1998**, *19*, 1639.
31. Park, H.; Lee, J.; Lee, S. *Proteins* **2006**, *65*, 549.
32. Jeffrey, G. A. *An Introduction to Hydrogen Bonding*; Oxford University Press: Oxford, 1997.
33. Lipinski, C. A.; Lombardo, F.; Dominy, B. W.; Feeney, P. J. *Adv. Drug. Delivery Rev.* **1997**, *23*, 3.
34. Gasteiger, J.; Marsili, M. *Tetrahedron* **1980**, *36*, 3219.
35. Park, H.; Jeon, J. H. *Phys. Rev. E* **2007**, *75*, 021916.
36. Stouten, P. F. W.; Frömmel, C.; Nakamura, H.; Sander, C. *Mol. Simul.* **1993**, *10*, 97.
37. Kang, H.; Choi, H.; Park, H. *J. Chem. Inf. Model.* **2007**, *47*, 509.
38. Shoichet, B. K.; Leach, A. R.; Kuntz, I. D. *Proteins* **1999**, *34*, 4.
39. Roujeinikova, A.; Raasch, C.; Sedelnikova, S.; Liebl, W.; Rice, D. W. *J. Mol. Biol.* **2002**, *321*, 149.
40. Zhou, J.-M.; Zhou, J.-H.; Meng, Y.; Chen, M.-B. *J. Chem. Theory Comput.* **2006**, *2*, 157.